2024 IEEE International Conference on Robotics and Automation (ICRA 2024)
May 13-17, 2024. Yokohama, Japan

Design of A Rigid-soft Hybrid Robotic Glove with Force Sensing Function

Hexin Li, Li Jiang*, Ruichen Zhen, Ming Cheng and Kehan Ding

Abstract— **Soft robotic gloves can not only provide timely, effective, safe and cheap rehabilitation training for patients with impaired movement function of hand, but also assist in completing daily grasping activities. However, most soft robotic gloves are completely composed of flexible structures. Although they have high flexibility and safety, there are problems such as poor fit and low output force. In order to solve these problems, this paper refers to the structure of the human hand and designs an articulated rigid-soft hybrid robotic glove, which combines the advantages of rigid robotic gloves and soft robotic gloves, and has high flexibility, high output force and good fit. In addition, soft robotic gloves generally lack the ability to sense the force between the human hand and the glove. Therefore, this paper designed an array flexible force sensor, and studied the structure, signal acquisition and preparation process of the sensor. Finally, a complete test platform was built to test the performance of the rigid-soft hybrid robotic glove with force sensing function. The test results show that the robotic glove has good fit and high output force, can effectively assist training and assist grasping, and can perceive the contact force.**

I. Introduction

Clinically, there are many patients with partial or total loss of hand function, limited finger range of motion and insufficient finger muscle strength caused by diseases or accidents such as cerebrovascular accident, rheumatoid arthritis and spinal cord injury [1]. There are a large number of patients with hand motor dysfunction in the world. Cerebrovascular accident is one of the main causes of this problem, which has a serious impact on the motor function of limbs, including hand motor function [2], [3].

As one of the important organs for human interaction with the outside world, the hand can not only complete various complex movements, but also the sensory organs of the hand are an important way for humans to perceive the world. Therefore, rehabilitation training for patients with hand motor dysfunction is extremely important. Positive and correct training is helpful to the reconstruction of human hand motor function [4]. Any device that can help restore hand function or assist in daily grasping activities is of positive significance for improving the quality of life of patients [5], [6]. The emergence of robotic gloves is expected to improve the recovery rate and quality of life of patients with hand motor dysfunction.

Early robotic gloves mostly use rigid structures and are driven by motors or micro-cylinders [7]-[12]. Although they have high accuracy, they are expensive, heavy, inconvenient to carry and have poor interaction with human hands, making it unsuitable for home rehabilitation training [13], [14]. With the rise of soft robot technology and the development of new soft materials and new processes, researchers have used soft materials for the production of robotic gloves [15]-[26]. The soft robotic gloves have gradually replaced the rigid robotic gloves because of their portability, safety and low cost. It has become a research hotspot. However, most of the soft robotic gloves are composed entirely of soft structures, which have disadvantages problems such as poor fit and low stiffness. In addition, the existing soft robotic gloves generally lack force sensing function. They cannot detect the output force in real time, and cannot achieve rehabilitation training through force control.

In this paper, the advantages of rigid and soft robotic gloves are combined, and an articulated rigid-soft hybrid robotic glove (Fig. 9) is designed with reference to the human hand structure. First, this paper designed the structure of the robotic glove and established a kinematic model. Then, this paper designed an array-type flexible force sensor to provide force sensing for the robotic glove. Finally, this paper completed the integration of the structure of each part of the robotic glove, and designed a set of drive and control system. A set of performance test system for the rigid-soft hybrid robotic glove was built, and the performance of the robotic glove was tested using this test system. The test results show that the robotic glove has a good fit with the human hand, the joints and fingertips have high output force and can realize the perception of the force.

II. Design of the Rigid-soft Hybrid Robotic Glove

In this section, through the research and analysis of the parameters and motion characteristics of the human hand, referring to the structure of the human hand, based on our previous study of the soft hand [27] structure, the overall structure of the rigid-soft hybrid robotic glove is designed, including the distribution of degrees of freedom, the design of joints and knuckles. The bending deformation of the articulated robotic glove is highly similar to that of the human hand, which can achieve a good fit with the human hand. Therefore, it can apply force to the human hand more effectively, so as to achieve better rehabilitation and assist effect.

A. Design and production of the robotic glove

The thumb of the rigid-soft hybrid robotic glove has two air chambers of metacarpophalangeal (MCP) and interphalangeal (IP). The other four fingers have three joint chambers: MCP, proximal interphalangeal (PIP) and distal interphalangeal (DIP), in which PIP and DIP are coupled. All joint air chambers are fiber reinforced structures, and a strain limiting layer is pasted on one side of the joint air chamber.

* Research supported by the National Natural Science Foundation of China (Grant No. 91948302, No. U1813209).

Hexin Li, Li Jiang, Ruichen Zhen, Ming Cheng and Kehan Ding are with State Key Laboratory of Robotics and System, Harbin Institute of Technology. (corresponding author: Li Jiang, e-mail: jiangli01@hit.edu.cn).

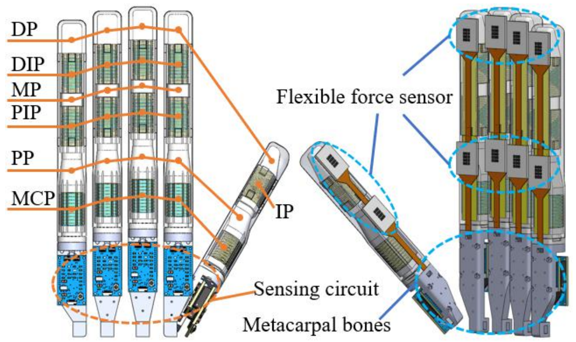

Figure 1. Structure of the robotic glove

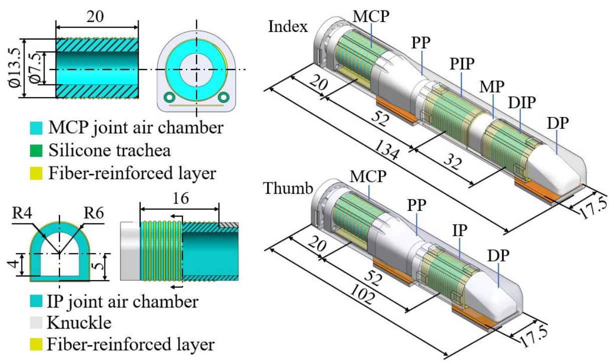

Figure 2. Finger structure and size

When inflated, the air chamber will bend to the side of the strain limiting layer. The air chambers of the fingers are connected by knuckles similar to human hand bones. There is a flexible force sensor at the proximal phalanx (PP) and distal phalanx (DP) knuckles of the finger, respectively. The metacarpal bones of the glove refer to the design of the five longest metacarpal bones of the human hand. The structure of the whole robotic glove is shown in Fig. 1.

The IP of the thumb is the same as the DIP and PIP structures of the other four fingers, collectively referred to as IP. The cross-section shape of the IP joint is a combination of semicircle and rectangle. The MCP joints of all fingers have the same structure. The cross-sectional shape of the MCP joint is circular. This is in order to reserve space for the placement of the silicone trachea for the ventilation of the IP joint. The silicone trachea is arranged at the bottom of the MCP chamber near the strain limiting layer, which can effectively reduce the influence of the trachea on the bending of the MCP joint. The design of the knuckle is completed by referring to the finger bone of the human hand, and the fingers of the mechanical glove are obtained after assembly, the finger structure is shown in Fig. 2.

The knuckles of rigid-soft hybrid fingers are made by 3D printing. Other structures of the finger are made by pouring silica gel into the 3D printed mold, heating, curing and demoulding. Compared with the single air chamber soft finger [28] shown in Fig. 3 (a) and the multiple air chambers soft finger [28] shown in Fig. 3 (b), the articulated rigid-soft integrated finger can achieve close fit with the human hand, as shown in Fig. 3 (c). It can not only reduce the fixed point between the glove and the human hand, improve the comfort, but also apply force to each joint more effectively, so as to achieve better rehabilitation and assist effect.

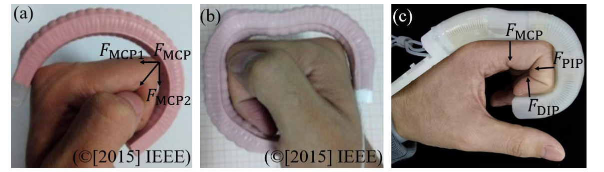

Figure 3. Comparison of the fit between fingers of different structures and human hands. (a) Single air chamber finger [28]. (b) Multiple air chambers finger [28]. (c) Articulated rigid-soft hybrid finger. All figures are reproduced with permission.

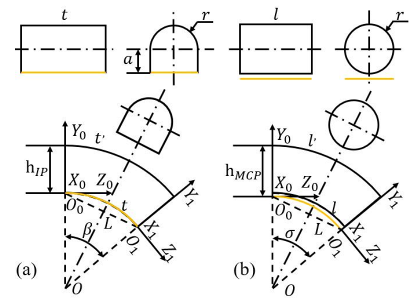

Figure 4. Kinematics model of the joints. (a) Kinematics model of IP. (b) Kinematics model of MCP

B. Kinematics model of the robotic glove

The kinematics model of the joint chamber is established based on the assumption of constant curvature bending and the assumption of constant chamber section (Fig. 4). The cross section of the IP joint is a combination of a semicircle with a radius of r and a rectangle with a height of a. The length of strain limiting layer is t. The bending angle when inflating is β. The coordinate system $O_0X_0Y_0Z_0$ and $O_1X_1Y_1Z_1$ are established on both sides of the end face of the strain limiting layer of the IP joint. The origin O is located in the middle of the strain limiting layer. The Z-axis is perpendicular to the end face towards the tip of the finger. The Y-axis is perpendicular to the bottom of the air chamber. The X-axis and the other two axes form the right-hand rule.

The value of the chord length L can be obtained by calculation:

$$L = 2\frac{t}{\beta}\sin\frac{\beta}{2} \tag{1}$$

Furthermore, it can be calculated that the moving distance of $O_1X_1Y_1Z_1$ relative to $O_0X_0Y_0Z_0$ along the Y_0-axis is $-t(1-\cos\beta)/\beta$, and the moving distance along the Z_0-axis is $t\sin\beta/\beta$. Finally, the transformation matrix between the two coordinate systems can be obtained:

$$ {}^{0}_{1}T_{IP} = \begin{pmatrix} 1 & 0 & 0 & 0 \\ 0 & c\beta & -s\beta & -t(1-c\beta)/\beta \\ 0 & s\beta & c\beta & ts\beta/\beta \\ 0 & 0 & 0 & 1 \end{pmatrix} \tag{2}$$

The cross section of the MCP joint is a circle with a radius of r. The length of strain limiting layer is l. The bending angle when inflating is σ. According to the derivation method of the kinematics of the IP joint, the coordinate transformation matrix can be obtained:

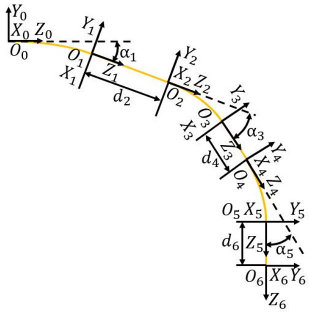

Figure 5. Kinematics model of the index finger

$$ {}^{0}_{1}T_{MCP} = \begin{pmatrix} 1 & 0 & 0 & 0 \\ 0 & c\sigma & -s\sigma & -l(1-c\sigma)/\sigma \\ 0 & s\sigma & c\sigma & ls\sigma/\sigma \\ 0 & 0 & 0 & 1 \end{pmatrix} \tag{3} $$

The kinematics model of the finger is established by taking the index finger as an example (Fig. 5). The coordinate system $O_iX_iY_iZ_i$ is established at the two ends of each joint and the fingertip of the index finger, where $i = 0,1,2,3,4,5,6$.

The forward kinematics equation is:

$$ {}^{0}T_i = {}^{0}T_1 \cdot {}^{1}T_2 \cdots {}^{i-1}T_i \tag{4} $$

The transformation matrices ${}^{0}T_1$, ${}^{2}T_3$ and ${}^{4}T_5$ between the coordinates of both ends of each joint have been derived in the part of joint kinematics. According to the conclusion, it can be seen that:

When i =1, it can be obtained by formula (3):

$$ {}^{0}T_1 = {}^{0}_{1}T_{MCP}(\alpha_1) \tag{5} $$

When i=3,5, it can be obtained by formula (2):

$$ {}^{i-1}T_i = {}^{0}_{1}T_{IP}(\alpha_i) \tag{6} $$

For the coordinates at both ends of the knuckle (i = 2,4,6), there is only a translation transformation between the two coordinate systems. The translation distance is d_i , which is the length of the knuckle, so the transformation matrix is:

$$ {}^{i-1}T_i = \begin{pmatrix} 1 & 0 & 0 & 0 \\ 0 & 1 & 0 & 0 \\ 0 & 0 & 1 & d_i \\ 0 & 0 & 0 & 1 \end{pmatrix} \tag{7} $$

III. FORCE SENSING DESIGN OF THE ROBOTIC GLOVE

At present, many studies have integrated position sensors on soft robotic gloves [20]-[24], trying to achieve good rehabilitation effects with accurate position control. However, rehabilitation training is a dynamic process, and the maximum bending position suitable for the next stage can only be predicted, which is difficult. If the output force can be monitored in real time and adjusted according to the needs of different rehabilitation stages to ensure that each bending ends with an appropriate output force, better rehabilitation results can be achieved. However, there are few studies on integrating

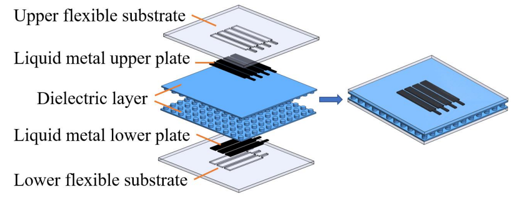

Figure 6. The structure of flexible force sensor

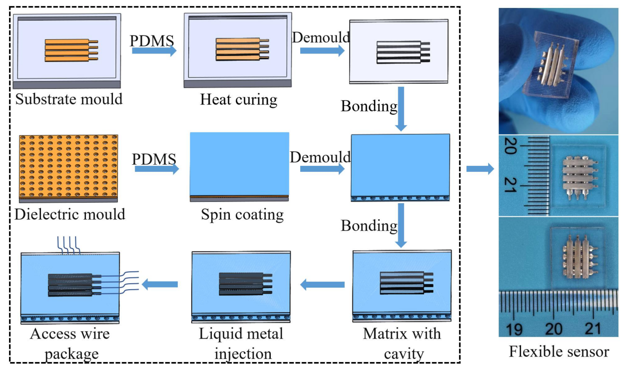

Figure 7. Flexible force sensor and its preparation process

flexible force sensors on soft robotic gloves. Some studies have integrated flexible force sensors on sensing gloves for mirror therapy [25] and virtual reality rehabilitation systems [26]. Therefore, we designed a flexible force sensor and integrated it into the glove to directly measure the force exerted by the rehabilitation glove on the fingers. The sensor is designed into an array to achieve multi-point measurement and output the maximum value among multiple measurement values in real time to measure the maximum output force.

A. Design and fabrication of flexible force sensor

The flexible force sensor is based on the principle of parallel plate capacitance. The structure of the sensor (Fig. 6) from top to bottom is: upper flexible substrate, upper electrode layer, dielectric layer with cylindrical microstructure, lower electrode layer and lower flexible substrate.

The preparation process of the sensor can be divided into the preparation of the flexible substrate, the preparation of the intermediate dielectric layer, the bonding between the layers of the sensor and the injection of the liquid metal plate (Fig. 7). Soft lithography, spin coating and plasma bonding are mainly used.

The material of the liquid metal plate is Eutectic Gallium-Indium, and the materials of other parts are Polydimethylsiloxane (PDMS). The flexible sensor (Fig. 7) consists of 3×4 array units, each unit size is 1.5×1.5mm, and the center distance between adjacent array units is 2mm. The overall size is about 15×13mm. The total thickness of the sensor is about 2mm.

B. Design of sensor signal acquisition circuit

The flexible sensor contains multiple array units. In order to collect the capacitance value of each array unit, a row-column gating circuit needs to be designed. The sensor signal acquisition circuit is mainly composed of microcontroller unit (MCU), capacitance digital conversion module and row-column gating module. The block diagram of the signal acquisition circuit is shown in Fig. 8.

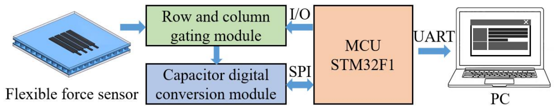

Figure 8. Block diagram of sensor signal acquisition circuit

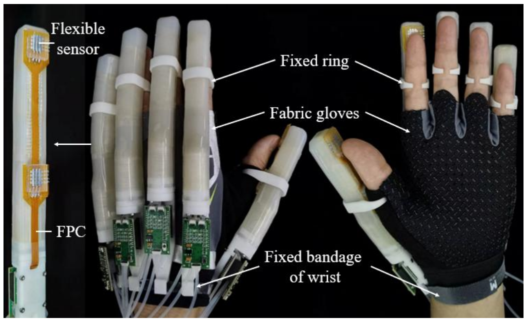

Figure 9. The rigid-soft hybrid robotic glove with force sensing function

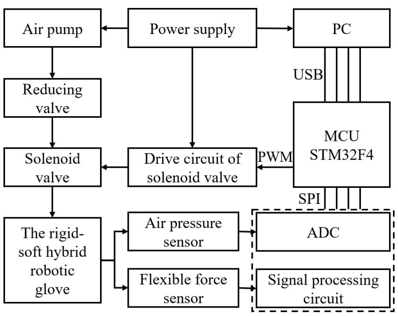

Figure 10. Drive and control system of the robotic glove

IV. The Integration of the Robotic Glove and the Design of Its Control and Drive System

After completing the design and manufacture of fingers and the flexible force sensor, we integrate all parts together to make a complete mechanical glove. In order to realize the drive of the robotic glove, we designed its control and drive system.

A. *Integration of the robotic glove*

After the manufacture of the finger and the flexible force sensor of the robotic glove, a flexible force sensor is pasted on the bottom of the MP and DP of the finger respectively. The deformation of the glove at these positions during movement is very small, which can reduce the influence of deformation such as stretching and bending on the sensor measurement and ensure the measurement accuracy. The sensor is used to measure the output force of MCP joint and IP joint.

The five metacarpal bones of the robotic glove are sewn on the stretchable fabric glove, and the sensor signal acquisition circuit is fixed on the metacarpal bone. Finally, we get a complete robotic glove (Fig. 9). The robotic glove and the human hand are fixed by the fabric glove, the fixed ring and the fixed bandage of wrist. The reliable fixation between the glove and the human hand is realized with fewer fixed points, which greatly improves the wearing comfort.

B. *Design of control and drive system for the robotic glove*

The drive and control system of the robotic glove (Fig. 10) is mainly composed of MCU, pneumatic circuit, sensing system and drive circuit. The MCU controls the pneumatic circuit to inflate and deflate the robotic gloves. The air pressure sensor in the circuit feeds back the pressure value in the air chamber to the controller to realize feedback adjustment of the pressure in the air chamber. The force sensing function is realized through the pressure value fed back by the flexible force sensor.

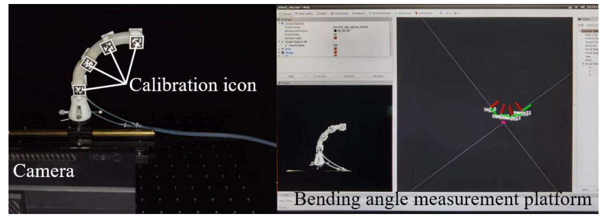

Figure 11. Bending angle test experiment

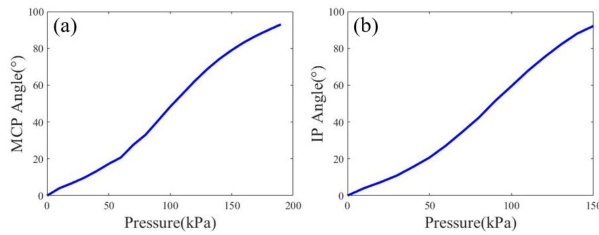

Figure 12. Bending angle on (a) MCP and (b) IP joint under different input air pressure

Each finger of the robotic glove has two active degrees of freedom, and the whole glove has a total of 10 active degrees of freedom. Therefore, the whole hardware execution loop needs to have the ability to generate these 10 degrees of freedom, so as to realize the inflation and deflation of the MCP joint air chamber and the IP joint air chamber of each finger respectively. In this paper, each joint air chamber is equipped with two high-speed solenoid valves to control inflation and deflation respectively. The pneumatic circuit is mainly composed of air pump, pressure reducing valve, digital pressure gauge, solenoid valve and gas pipe.

The robotic glove is connected with the drive and control system to complete the construction of the robotic glove performance test system (Fig. 16). The test system can control the inflation and deflation of the robotic gloves through the upper computer, and drive the robotic gloves to complete the expected movement.

V. Performance of the Robotic Glove

This paper has established a sensor performance test platform and a rigid-soft hybrid robotic glove performance test system to test the performance of the robotic glove and the flexible force sensor.

A. *Bending performance of the robotic glove*

In order to test the bending ability of the fingers of the robotic glove, we use our laboratory's vision-based bending angle measurement platform (The detection error is no more than 0.5°) to measure the bending angle of MCP and IP joints under pressure. As shown in Fig. 11, the proximal end of the finger is fixed vertically to reduce the influence of gravity on the bending angle. The MCP and IP joints of the finger were increased by air pressure from 0 kPa, and the air pressure was increased by 10 kPa each time until the finger bending angle exceeded 90°.

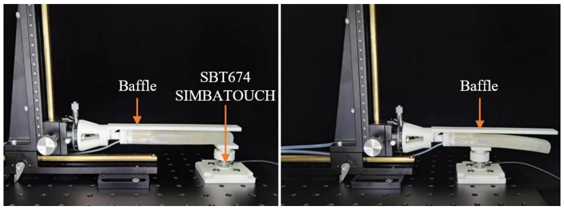

Figure 13. Finger output force test experiment

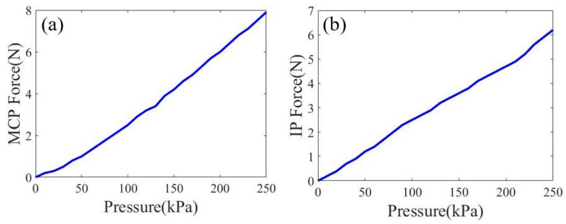

Figure 14. The output force of the (a) MCP and (b) IP under different input air pressure

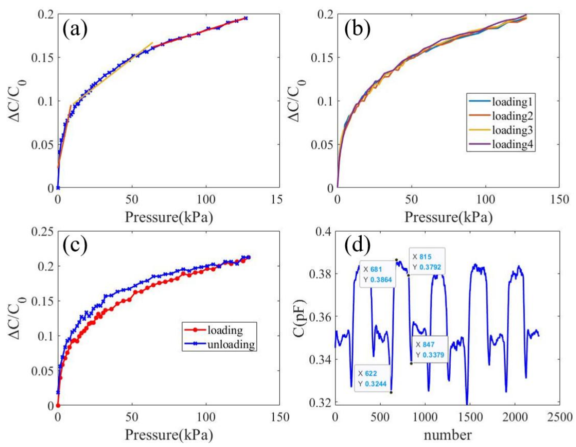

Figure 15. Performance the sensor. (a) Sensitivity curve. (b) Repeating accuracy curve. (c) Hysteresis curve. (d) Dynamic response curve.

The results show that the bending angle of the joint chamber increases nonlinearly with the input pressure. At 180 kPa, the bending angle of the MCP joint exceeds 90°, as shown in Fig. 12 (a); at 140 kPa, the bending of the IP joint exceeds 90°, as shown in Fig. 12 (b).

B. Output force performance of the robotic glove

In the experiment, commercial pressure sensors (SBT674, SIMBATOUCH) were used to measure the output forces of MCP joint and IP joint, as well as the maximum output forces of thumb fingertip and index fingertip. Firstly, the proximal end of the finger is fixed horizontally, and the contact force between the finger and the sensor is just zero. From 0 kPa to 250 kPa, the pressure value of the commercial pressure sensor was recorded.

The relationship between the output force of the MCP joint and the IP joint and the input air pressure is obtained, as shown in Fig. 14. From the results, it can be seen that the relationship between the joint output force and the input air pressure is approximately linear. At 250 kPa, the output forces of the MCP joint and the IP joint are 7.9 N and 6.2 N, respectively. The MCP and IP joints of the fingers were simultaneously pressurized to 250 KPa, and the fingertip output forces of the

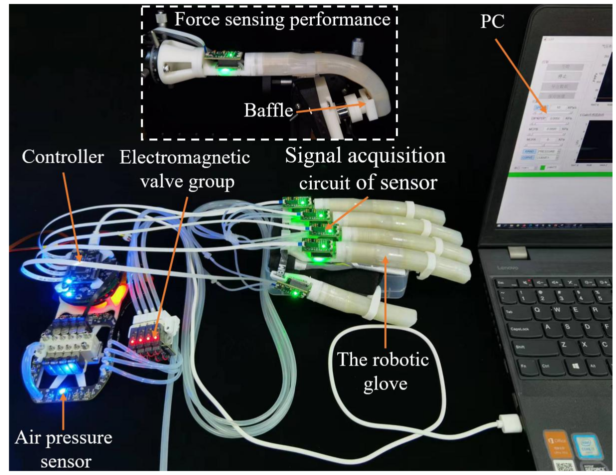

Figure 16. Force sensing experiment of the robotic glove

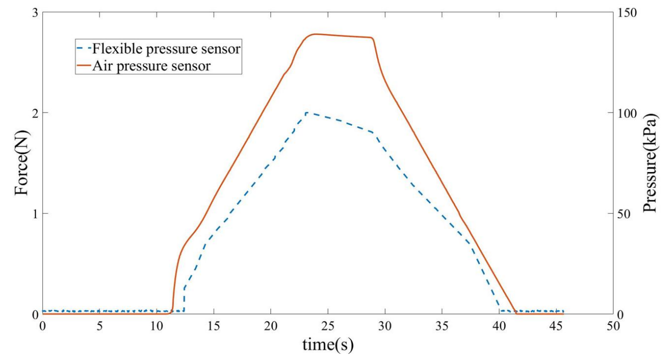

Figure 17. The Result of force sensing experiment

index finger and the thumb were 7.8N and 6.0N, respectively. It can be seen that the robotic glove has a high output force and can effectively drive the human hand movement.

C. Force sensing performance of the robotic glove

Firstly, we tested the sensitivity, repeatability, hysteresis characteristics and dynamic response of the sensor. The test results are shown in Fig. 15.

The sensitivity curve of the sensor is segmented and fitted, and the segmented sensitivity and linearity are: 0.0101 kPa^{-1}, 26.8%; 0.0013 kPa^{-1}, 12.2% and 0.0005 kPa^{-1}, 5.8%, respectively. It can be seen that the sensor has high sensitivity in a small pressure range. As the pressure increases, the sensitivity gradually decreases, but the linearity gradually increases. In addition, the sensor has high repeatability (3.87%) and short dynamic response time (< 50ms). The hysteresis error of the sensor is 10.85%.

In this paper, flexible force sensors are installed on the fingers of the glove to detect the output force. We use a finger to verify that the robotic glove has the ability to sense force. We placed a baffle under the finger of the robotic glove, and pressurized the finger of the robotic glove to 140 kPa from 0 kPa. After holding for a period of time, the air pressure was reduced to 0 kPa. The robotic glove was in contact with the baffle during the pressurization process, resulting in contact force. The flexible force sensor measures and returns the force information. The experimental device is shown in Fig. 16.

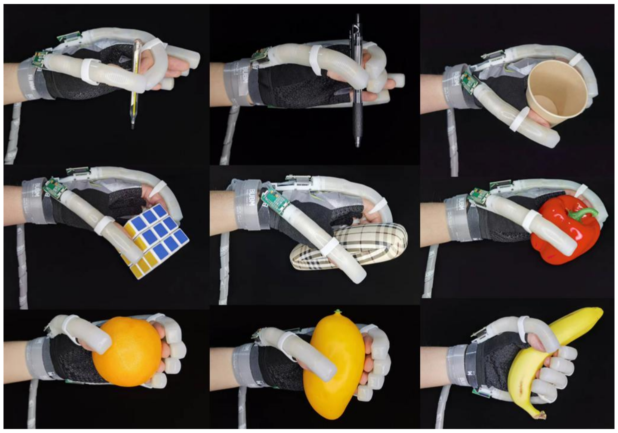

Figure 18. The robotic glove assists the human hand to grab a variety of daily necessities.

The feedback curves of the flexible force sensor and the air pressure sensor are shown in Fig. 17. From the results, it can be seen that with the increase of air pressure, the output force of the glove detected by the flexible force sensor is gradually increasing. When the air pressure decreases, the output force detected by the flexible force sensor also decreases. This experiment shows that the flexible force sensor can detect and feedback the output force of the robotic glove in real time.

D. Assisted grasping performance of the robotic glove

Wearing the robotic glove to grasp some daily necessities to verify its ability to assist in grasping. Through the experimental results (Fig. 18), it can be concluded that the robotic glove can assist the human hand to grasp objects of different shapes by driving two, three or five fingers of the human hand. In the process of grasping, the glove can always fit the human hand well and can effectively play a role in assisting.

VI. Conclusion

In this paper, a rigid-soft hybrid robotic glove with force sensing function is designed. The robotic glove refers to the structure of human hand, which is composed of rigid knuckle, flexible matrix and soft drive joint. In addition, this paper also developed a stretchable array flexible force sensor to provide force sensing function for the robotic glove. Finally, this paper establishes a sensor performance test platform and a rigid-soft hybrid robotic glove performance test system. The test shows that each joint and fingertip of the glove have a high output force. The joint design of the rigid-soft hybrid structure makes it have a good fit with the human hand, which can more effectively complete the rehabilitation training and assist the human hand to complete the grasping activity. The flexible force sensor on the glove has high repeatability accuracy, fast response time, high sensitivity in the low-pressure detection range, and can perceive and feedback the output force of the robotic glove. The glove has a good application prospect in hand robotic training and assisted grasping.

In the future, we will optimize the structure, control and flexible force sensor signal of the robotic glove on the basis of this research. For example, optimizing the size of the robotic glove, reducing the weight of the robotic glove, realizing the force feedback control of the robotic glove and the rehabilitation training based on the target force.

References

[1] Tiboni, Monica, and Cinzia Amici, "Soft Gloves: A Review on Recent Developments in Actuation, Sensing, Control and Applications," *Actuators*, vol. 11, no. 8, pp. 232, August 2022.

[2] D. Popescu, M. Ivanescu, R. Popescu, L. -C. Popescu, A. Petrisor and A. -M. Bumbea, "Post-stroke assistive rehabilitation robotic gloves," *International Conference and Exposition on Electrical and Power Engineering (EPE)*, Iasi, Romania, 2016, pp. 360-365.

[3] P. Langhorne, J. Bernhardt, G. Kwakkel, "Stroke rehabilitation," *The Lancet*, vol. 377, pp. 1693–1702, May 2011.

[4] A. N. Krichevets, E. B. Sirotkina, I. V. Yevsevicheva, and L. M Zeldin, "Computer games as a means of movement rehabilitation," *Disability & Rehabilitation*, vol. 17, no. 2, pp. 100-105, 1995.

[5] C. K. Andersen, K. U. Wittrup-Jensen, A. Lolk, et al. "Ability to perform activities of daily living is the main factor affecting quality of life in patients with dementia," *Health Qual Life Outcomes*, vol. 2, pp. 52, September 2004.

[6] Paola, Colombo, and Giovanni, et al. "Lower Tinetti scores can support an early diagnosis of spatial neglect in post-stroke patients," *European journal of physical and rehabilitation medicine*, vol. 55, no. 6, pp.722-727, 2019.

[7] M. Bouzit, G. Burdea, G. Popescu and R. Boian, "The Rutgers Master II-new design force-feedback glove," in *IEEE/ASME Transactions on Mechatronics*, vol. 7, no. 2, pp. 256-263, June 2002.

[8] M. DiCicco, L. Lucas and Y. Matsuoka, "Comparison of control strategies for an EMG controlled orthotic exoskeleton for the hand," *IEEE International Conference on Robotics and Automation*, New Orleans, LA, USA, 2004, pp. 1622-1627, vol.2.

[9] A. Wege and A. Zimmermann, "Electromyography sensor based control for a hand exoskeleton," *2007 IEEE International Conference on Robotics and Biomimetics (ROBIO)*, Sanya, China, 2007, pp. 1470-1475.

[10] M. Cempini, M. Cortese and N. Vitiello, "A Powered Finger–Thumb Wearable Hand Exoskeleton With Self-Aligning Joint Axes," in *IEEE/ASME Transactions on Mechatronics*, vol. 20, no. 2, pp. 705-716, April 2015.

[11] YANG J, XIE H, SHI J. "A novel motion-coupling design for a jointless tendon-driven finger exoskeleton for rehabilitation," *Mechanism and Machine Theory*. pp. 83-102, vol. 99, May 2016.

[12] D. Wang, Q. Meng, Q. Meng, X. Li and H. Yu, "Design and Development of a Portable Exoskeleton for Hand Rehabilitation," in *IEEE Transactions on Neural Systems and Rehabilitation Engineering*, vol. 26, no. 12, pp. 2376-2386, Dec. 2018.

[13] Proulx CE, Beaulac M, et al. "Review of the effects of soft robotic gloves for activity-based rehabilitation in individuals with reduced hand function and manual dexterity following a neurological event," *J Rehabil Assist Technol Eng*, vol. 7, May 2020.

[14] T. Du Plessis, K. Djouani, and C. Oosthuizen, "A review of active hand exoskeletons for rehabilitation and assistance," *Robotics*, vol. 10, no. 1, pp. 40, May 2021.

[15] P. Polygerinos et al. "Towards a soft pneumatic glove for hand rehabilitation," 2013 *IEEE/RSJ International Conference on Intelligent Robots and Systems*, Tokyo, Japan, 2013, pp. 1512-1517.

[16] Polygerinos P, Wang Z, Galloway K, et al. "Soft robotic glove for combined assistance and at-home rehabilitation," *Robotics & Autonomous Systems*. vol. 73, no. 2015, pp. 135-143.

[17] H. K. Yap et al. "A fully fabric-based bidirectional soft robotic glove for assistance and rehabilitation of hand impaired patients," in *IEEE Robotics and Automation Letters*, vol. 2, no. 3, pp. 1383-1390, July 2017.

[18] T. Jiralerspong, K. H. L. Heung, R. K. Y. Tong and Z. Li, "A Novel Soft Robotic Glove for Daily Life Assistance," *2018 7th IEEE International Conference on Biomedical Robotics and Biomechatronics (Biorob)*, Enschede, Netherlands, 2018, pp. 671-676.

[19] J. Wang, Y. Fei and W. Pang, "Design, Modeling, and Testing of a Soft Pneumatic Glove With Segmented PneuNets Bending Actuators," in *IEEE/ASME Transactions on Mechatronics*, vol. 24, no. 3, pp. 990-1001, June 2019.

[20] Sui, M., Ouyang, Y., Jin, H. et al. A soft-packaged and portable rehabilitation glove capable of closed-loop fine motor skills. *Nat Mach Intell* 5, 1149-1160 (2023).

[21] Zhu, Yinlong, Weizhuang Gong, Kaimei Chu, Xu Wang, Zhiqiang Hu, and Haijun Su. 2022. "A Novel Wearable Soft Glove for Hand Rehabilitation and Assistive Grasping" *Sensors* 22, no. 16: 6294.

[22] S. Ganeson, R. Ambar and M. M. A. Jamil, "Design of a low-cost instrumented glove for hand rehabilitation monitoring system," *2016 6th IEEE International Conference on Control System, Computing and Engineering (ICCSCE)*, Penang, Malaysia, 2016, pp. 189-192.

[23] Dong Hyun Kim, S. W. Lee and Hyung-Soon Park, "Sensor evaluation for soft robotic hand rehabilitation devices," *2016 6th IEEE International Conference on Biomedical Robotics and Biomechatronics (BioRob)*, Singapore, 2016, pp. 1220-1223.

[24] Meng, Fanye, Chang Liu, Yu Li, Hao Hao, Qishen Li, Chenyi Lyu, Zimo Wang, Gang Ge, Junyi Yin, XiaoqiangJi, and et al. 2023. "Personalized and Safe Soft Glove for Rehabilitation Training" *Electronics* 12, no. 11:2531.

[25] X. Chen et al. "A Wearable Hand Rehabilitation System With Soft Gloves," in *IEEE Transactions on Industrial Informatics*, vol. 17, no. 2, pp. 943-952, Feb. 2021.

[26] S.-C. Yeh, S.-H. Lee, R.-C. Chan, S. Chen, and A. Rizzo, "A virtual reality system integrated with robot-assisted haptics to simulate pinch-grip task: Motor ingredients for the assessment in chronic stroke," *NeuroRehabilitation*, vol. 35, no. 3, pp. 435-449, 2014.

[27] Ruichen Zhen, Li Jiang, Hexin Li, and Bangchu Yang. "Modular Bioinspired Hand with Multijoint Rigid-Soft Finger Possessing Proprioception," *Soft Robotics*, vol. 10, no. 1, pp. 380-394, Apr 2023.

[28] J. Zhang, H. Wang, J. Tang, H. Guo and J. Hong, "Modeling and design of a soft pneumatic finger for hand rehabilitation," *2015 IEEE International Conference on Information and Automation*, Lijiang, China, 2015, pp. 2460-2465.